Internet of Things 11 (2020) 100265

Contents lists available at ScienceDirect

Internet of Things

journal homepage: www.elsevier.com/locate/iot

Customized novel routing metrics for wireless mesh-based swarm-of-drones applications☆

Oscar Bautista*, Kemal Akkaya, A. Selcuk Uluagac

Department of Electrical and Computer Engineering, Florida International University Miami, FL, 33174, USA

ARTICLE INFO

Article history:
Received 26 March 2020
Revised 25 July 2020
Accepted 26 July 2020
Available online 29 July 2020

Keywords:
IoT
MANET
Flying adhoc network
802.11s
HWMP
Airtime routing metric
Link quality metric
Swarm-of-drones
Mobility model
Throughput
End-to-end delay

ABSTRACT

With the proliferation of drones, there is an increasing interest on utilizing swarm-of-drones in numerous applications from surveillance to search and rescue. While a swarm-of-drones (a.k.a flying ad hoc networks (FANETs)) is essentially a special form of mobile ad-hoc networks (MANETs) which has been studied for many years, there are unique requirements of drone applications that necessitate re-visiting MANET protocols. These challenges stem from 3-D environments the drones are deployed in, and their specific way of mobility which adds to the wireless link management challenges among the drones. To tackle these challenges, in this paper, we propose adopting the current mesh standard, namely IEEE 802.11s, in its routing capabilities to provide improved performance. Specifically, we propose two new link quality routing metrics called SrFTime and CRP as an alternative to the IEEE 802.11s default Airtime routing metric to meet network throughput requirements for FANET applications. Basically, SrFTime improves network performance of stationary FANETs, while CRP is designed to fit the transient link characteristics of mobile drones and enable more efficient routes from drones to their destinations. To be able to test these metrics, we also introduce a group mobility model adaptation for FANET's needs. The evaluations in the actual 802.11s standard using ns-3 simulator and introduced 3-D mobility models indicate that our proposed metrics outperform the existing one consistently under various conditions.

1. Introduction

In recent years, Unmanned Aerial Vehicles (UAV) or drones have been used in many military and civilian applications such as search and rescue operations, detection and tracking, intelligent transportation systems, managing wildfire, relay deployment, and logistics operations [1,2]. The trend in those applications indicates that typically a swarm of small-size UAVs are deployed due to its advantages for handling various tasks in coordination, when compared to a single large-size UAV in terms of cost, scalability, survivability, the speed of task completion, and small cross-section coverage [1]. In such applications drones carry sensors or can be in touch with other IoT devices in the environment for various tasks.

A swarm of drones is sometimes referred to as Flying Ad-hoc networks (FANET), which is synonymous to Mobile Ad-hoc Networks (MANET) that have been studied heavily in the past [3,4]. However, there are a number of differences which

☆ A very preliminary version of this work titled "A Novel Routing Metric for IEEE 802.11s-based Swarm-of-Drones Applications" has appeared in the proceedings of 16th EAI International Conference on Mobile and Ubiquitous Systems: Computing, Networking and Services (MobiQuitous) (2019) 514–521, doi:10.1145/3360774.3368197, In press.

* Corresponding author.
E-mail address: obaut004@fiu.edu (O. Bautista).

https://doi.org/10.1016/j.iot.2020.100265
2542-6605/

distinguish FANETs as a subset of MANETs while they certainly share many similar characteristics. For instance, FANETs typically have a much higher mobility with unpredictable movements that may result in frequent topology changes, while "MANET nodes usually have very low mobility" [5]. In a FANET, UAVs may be equipped with multiple sensors to collect data from their surrounding and then relay it to a control center [6,7] which is akin to wireless sensor networks (WSNs) [8]. Consequently, besides supporting peer-to-peer communications among drones for coordination and cooperation to maintain the network formation, FANETs also need to support data traffic that may require different data delivery strategies or quality of service (QoS) requirements. Furthermore, FANETs may also need to operate in a rapidly changing environment in 3-D terrain settings, from close to the ground up to high in the sky. 3-D settings are interesting as they may influence the number of links and interference among different nodes. Thus, to support reliable and stable FANET operations in various settings including urban and rural environments, MANET standards/protocols may not be directly applied.

One of such example MANET cases is when drones need to communicate with each other (i.e., meshing among each other) when they cannot communicate with an existing ground infrastructure or when such infrastructure is not available [7]. In such cases, for supporting multi-hop meshing among drones, routing protocols are needed. As this has been a vast area of research for MANETs and some standards such as IEEE 802.11s [9], Zigbee, etc. are already developed, they can be deployed for the same purpose in FANETs. Particularly, 802.11s standard suits the high data needs of drones as opposed to Zigbee or others. In addition, Wi-Fi dongles to run IEEE 802.11s are already available and they are convenient to use without any additional effort. Indeed, recently, this protocol was included in Google's WiFi routers as well [10].

However, IEEE 802.11s was not designed specifically for FANETs. It was mainly geared for stationary WiFi nodes that can form a wireless mesh network (WMN) to access the infrastructure. In a sense, it gives nodes the capability to do multi-hopping if one-hop communication to an access point (AP) is not available. Nevertheless, the existing works on drone routing [6,7,11] use the IEEE 802.11s standard as is which do not take into account the 3-D nature and abrupt link changes in such topologies. The way routes are determined is based on a certain routing metric called *Airtime* using an advanced on-demand distance vector (AODV)-like [12] routing protocol called Hybrid Wireless Mesh Protocol (HWMP) [9]. Basically, *Airtime* metric is derived from the time resources used by a specific link to send a test packet across the link and the average frame error rate on the same link.

In this paper, we argue that this current metric for HWMP routing does not fit well to FANETs due to their special challenges and requirements. Indeed, the main research gap for FANETs is that there is neither a specific routing protocol nor a routing metric designed and also deployed for their applications. Lack of access to 3D testing environments and actual drones make it even more challenging to deal with these problems within the FANET context. Therefore, specific research questions that can be mapped to these issues are: 1) How can we design a FANET-specific routing metric that will incorporate 3D terrain, mobility and propagation issues? and 2) How can we offer realistic 3D mobility models to be able to test this routing metric's performance along with other related metrics for routing?

We therefore propose a new routing metric that will best suite the needs of FANETs. The first improvement to the existing metric is called *Square Root Frame Time* (*SrFTime*) which is computed by using the existing *Probe* packets in IEEE 802.11s standard. Basically, we redefine the combination of time resources, error fluctuation and interference of links in 3-D environments to this new metric to improve certain QoS performance such as network throughput. Since the new metric does not require additional communication, no network overhead is added making this a cost-efficient routing metric too. Next, we built upon this metric to derive a *Comprehensive Radio and Power (CRP)* metric optimized for mobility. *CRP* minimizes some of the negative effects of link breakage due to mobility of drones that include increased packet bufferization and delay while a path repair is completed. CRP influences the metric value of links to nodes that are close to the transmission range coverage limit based on received power level measurements in an attempt to use alternative and more stable routes preferable over the current routes before a link break occurs.

We incorporated the proposed *SrFTime* and *CRP* into 802.11s mesh standard at the MAC layer in ns-3 network simulator. We then evaluated the performance of the revised IEEE 802.11s in 3-D mobile FANET topologies that we built based on a proposed group mobility model. This model was adapted from an existing reference point group mobility model to accommodate the characteristics of drones in a swarm. The results under a variety of conditions indicate that our proposed metrics consistently outperforms the original airtime metric in both stationary and mobile FANET topologies and *CRP* metric turns out to be a viable option for practical deployment.

This paper is organized as follows: Section 2 briefly describes previous work related to routing, routing metrics and FANET mobility models. Section 3 talks about the system model considered and key background information about 802.11s standard. Section 4 describes the modifications proposed to original Airtime metric, presenting our SrFTime metric, which is then optimized in Section 5 to derive CRP for FANET applications. We dedicate Section 7 to propose a new mobility model as a key aspect of effective FANET simulation. Section 8 presents the simulation results comparing the different routing metrics under different scenarios. Finally, Section 9 presents the conclusions of this work supported by the simulation results and future research direction.

2. Related work

There has been a lot of studies on routing and routing metrics for MANETs and WSNs to improve the performance. In this section, we summarize them to compare with what we are proposing.

2.1. Routing in mobile wireless networks

Routing in MANETs and Vehicular Adhoc Networks (VANETs) have been widely studied [13,14]. However, both of these types of wireless network have different routing requirements and challenges. They are not designed for 3-D environments, their mobility patterns and speeds are different and their data patterns are specific. Therefore, they need to be adapted for FANETs.

Arafat and Moh [15] wrote a comprehensive survey of routing protocols for UAV networks. However, many of those are known routing protocols for MANET which are not inherently suitable for FANET. The authors also include contributions specifically for FANET/UAV networks. Most of the testing-based simulations in these works use random mobility models while in our work we developed more appropriate mobile scenarios for FANET to better represent the characteristics of real UAV movements.

In a similar study, Nayyar [16] performed a comprehensive comparison of routing protocols for MANET such as AODV [12], DSDV [17], DSR [18], AOMDV [19], OLSR [20] and HWMP [9] when they are deployed for FANETs though the testing mobility model was not specified. The results for packet delivery ratio against node speed shows that HWMP outperformed the other routing protocols. Additionally, HWMP scored the highest throughput while sharing the least end-to-end delay performance with DSDV.

Due to the ability of HWMP to perform well for FANETs, we opted to improve its performance under a more realistic mobility model for 3-D FANET environments. In addition, it is already part of the IEEE 802.11s standard which has been implemented in practice.

2.2. General routing metrics

Routing metrics have been widely studied in many context for MANETs, WSNs and other similar networks. In this regard, Parissidis et al. [21] made a comprehensive survey and analysis of different routing metrics for WMN, categorizing them using different criteria such as the optimization goal including minimize delay, maximize network throughput among others. The authors also made distinctions in the way the information for metric computation is collected. In this study [21] the authors concluded that Expected Transmission Count (ETX) performs better than other metrics like Round Trip Time (RTT) and Per-hop Packet Pair (PktPair) since it is load-independent. Nonetheless, they also mention that since ETX does not take into consideration the transmission rate in multi-rate ad hoc wireless networks. Expected Transmission Time (ETT) was developed by adding to ETX a factor that included the size of a probing packet divided by the bandwidth of the link. Medium Time Metric (MTM) was designed independently around the same time by Awerbuch et al. [22], which is very similar to ETT differing only in that it includes control frames, back-off and fixed headers in the calculation of the link time usage, making MTM almost equivalent to the IEEE 802.11s' default Airtime metric. ETT and MTM throughput outperforms ETX especially in multi-rate ad hoc networks. In our work, since we consider 802.11-s-based FANETs, we propose improvements to Airtime metric to fit it to the requirements of FANETs.

2.3. Improvements to IEEE 802.11s

As our work involves revision to the existing IEEE 802.11s Airtime metric, we also summarize the literature on the improvements to this standard. The closest study to ours in this sense is reported in [23]. The authors propose a modification to 802.11s airtime link metric, considering the current link load in addition to the default elements used to compute the airtime. They basically propose new airtime metric values for different transmission rates and link load. However, there is no actual implementation or simulation that assesses the proposed improvement. Our purpose in this work is very much different as we seek to develop an improved metric that outperforms the current airtime metric in terms of network throughput specifically for FANET applications where we consider 3-D environments and dynamic nature of drone links.

2.4. Mobility models

MANET and VANET mobility models differ significantly from FANETs and this might cause a significant impact on the effectiveness of the proposed solutions since the evaluation results may differ considerably from real deployments. Bujari et al. [24] has noted the importance of using appropriate mobility models for FANET simulation. Similarly, Litvinov et al. [25] confirmed the same finding and also added coverage area and node density as important factors to consider for proper network operation. Specifically, group mobility models are more appropriate for FANET applications. However, to the best of our knowledge, there is no specific group mobility model designed for FANETs.

One of the group mobility models from the literature that might be adjusted for FANET simulation is Reference Point Group Mobility (RPGM) [26]. RPGM defines group of nodes where each group has its own mobility pattern and in each group there is a reference point, so that nodes belonging to that group will move pseudo randomly around this reference point with a defined maximum distance to it. Therefore, in this work, we chose RPGM to be adopted for swarm movement.

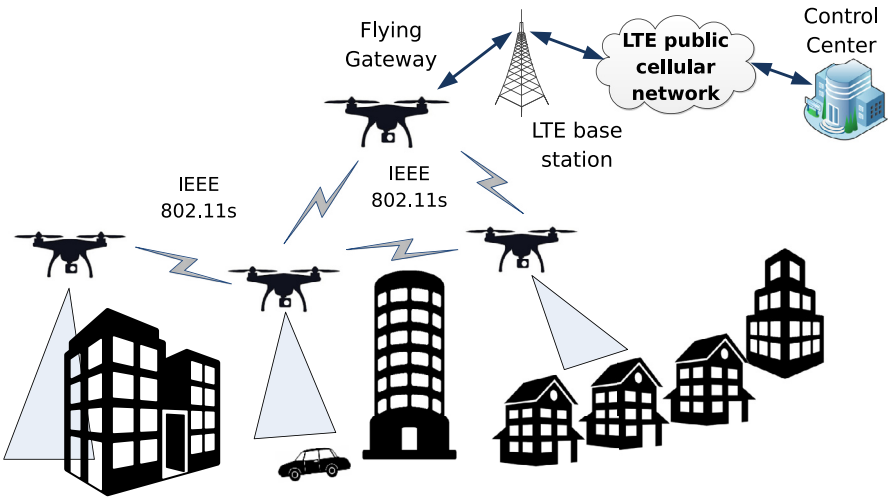

Fig. 1. Drone deployment in urban environment.

2.5. Application-specific drone implementations

Lastly, there are works on application-specific drone implementation, focused on improving a targeted task. For instance, Tropea et al. [27] evaluated the suitability of routing approaches inherited from MANET, specifically reactive flooding and link state routing for application on precision agriculture as well as the application-specific mechanisms to select other drone from the swarm to continue the task of another drone which is running out of power. Our work's focus is the general performance in terms of throughput and end-to-end delay using suitable 3-D mobility models.

3. Background and preliminaries

3.1. System model

We assume a swarm-of-drones or FANETs deployed for a mission in an area of interest, which could be either urban or rural. The drones are equipped with 802.11s radio communication interfaces. One of the drones in the swarm will be acting as the root, which is assumed to have long distance communication capabilities such as LTE to communicate with a control center, serving as a gateway for the 802.11s network. The drones may need to exchange data as well as relay data of each other to the gateway if the data needs to be communicated to a remote location. Fig. 1 exemplifies such scenario. For the rest of the paper, swarm and FANET are used interchangeably. Next, we provide some preliminaries before we explain our approach.

3.2. HWMP

HWMP is the default mandatory Routing Protocol for the 802.11s standard, though it allows vendors to implement any routing protocol and path metric as well [28]. HWMP supports two modes of operation: Reactive and Proactive modes, that can be used concurrently. The Reactive (On Demand) mode is adapted from AODV Routing Protocol [12], which initiates a path discovery when a station has a data to transmit. HWMP Path selection frames are used for path management. The basic frames are: *Path Request (PREQ), Path Reply (PREP)* and *Path Error (PERR)*. The first two are used for path discovery, while PERR is used to eliminate paths under specific conditions.

When a station needs to send data, it broadcasts a PREQ. Neighbors that are not the intended destination in turn will forward the PREQ to its neighbors propagating the PREQ throughout the network. The PREQ is updated at each station adding its new *link metric* value to compute a *path metric*. Note that the link metric is computed independently by each station. The stations receiving the PREQ that are not the intended destination could also send a PREP back to the station the PREQ was received from depending on the flags in the PREQ frame. PREP is a unicast frame. When the PREQ eventually reaches the intended destination, it sends a PREP back to the originator, following the same PREQ path. The best path (the one with the lower metric) is chosen at origin.

The proactive mode is used optionally. In this mode, one node in the network is chosen as the root node, which finds routes toward all nodes in the network by broadcasting proactive PREQs periodically. This way, when a node needs to send data to other stations, it first looks up the destination in its own routing table. If an entry does not exist for that destination, then it sends the data packet to the root node which relays the packet to the final destination. A combination of reactive and proactive modes enables efficient path selection in a wide variety of mesh networks [28].

Table 1
Airtime metric constants.

	IEEE 802.11a	IEEE 802.11b/g
O_{ca}	75μ; s	335μ; s
O_p	110μ; s	364μ; s

3.3. Airtime link metric

The 802.11s Wireless Mesh Standard uses *Airtime* as the default Routing Metric. According to the specification, the cost of a link that uses this metric has two main components: the time that would take a test frame to be sent through the link ($\frac{B_t}{r}$) and the average frame error rate of that link (e_{fr}) as shown in Eq. (1):

$$C_a = \left(O + \frac{B_t}{r}\right) \times \frac{1}{1 - e_{fr}}, \tag{1}$$

where O is the Physical Layer (PHY) dependent channel overhead that consists of the frame headers, training sequences, and access protocol frames. O is defined as $O = O_{ca} + O_p$, where O_{ca} is the channel access overhead, and O_p is the protocol overhead. Table 1 shows some Airtime Metric Constants for some of the 802.11 standards [29,30].

The parameter B_t is the size of the test frame in bits, whose default value is 8192 (or 1024 bytes), and r is the physical link rate.

The 802.11s standard does not define a specific method to calculate the frame error rate, e_{fr}. Rather, it is left to the specific implementation.

3.4. Propagation loss models

Propagation Loss Models are used to compute the receive (Rx) power level of the radio signal considering a specific environment. The two models we used for testing in this paper are briefly described below:

3.4.1. Friis propagation loss model

The Friis model [31] is valid only for propagation in free space within the so-called far field region. In practice, however, Friis is often used in scenarios where accurate propagation modeling is not deemed important.

3.4.2. ITU-R1411 LOS Propagation loss model

This model implements the ITU-R recommendation for Line-of-Sight (LoS) short range outdoor radio communication in the frequency range from 300 MHz to 100 GHz. This recommendation is based on the premise that propagation over paths of length less than 1 km is affected primarily by buildings and trees, rather than by variations in ground elevation. The effect of buildings is predominant since most short-path radio links are found in urban and suburban areas [32]. This is important for the cases of FANETs. The propagation behavior of these model is symmetric in the sense that they treat radio terminals at both ends of a path in the same manner. We chose this model since it accurately reflects the path loss in real environments.

4. Proposed routing metric for FANETs

4.1. Motivation

In IEEE 802.11s standard, the default Routing protocol HWMP, finds possible paths between a source and a destination then selects the best of them based on the metric also known as path cost. The path cost is calculated by adding the cost of each link along the way from source to destination and the preferred path is the one with the lower cost. As described in the previous section, the *Airtime* link metric quantifies the link quality based on the time it takes for a test frame to be transmitted through that link and weighted by the frame error rate. One link is preferred over another when its metric value (cost) is lower. Typically, a lower *Airtime* metric value is obtained when link speed is higher and frame error rate is lower.

However, airtime metric may not always be optimal for FANET applications. For instance, after close analysis of the effect of link rate in the airtime metric, we found that the discrete changes in the airtime link metric value due to a link rate change combined with specific average frame error rates may not result in a better throughput which is becoming more crucial for drone applications where video data collection, sensing, command&control are becoming very common.

Therefore, in this paper, we first introduce a revised routing metric called *SrFTime*, geared for increasing the FANET performance in terms of network throughput. For this purpose, we propose alternative ways to compute the average frame error rate and the link time usage as explained next. By using this metric, we expect that the network performs more efficiently by reducing collisions altogether.

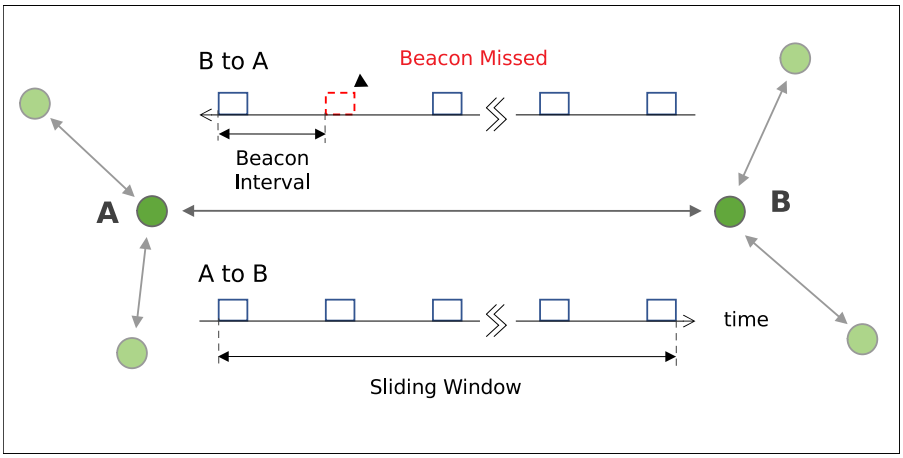

Fig. 2. Proposed frame error rate computation from Beacons.

4.2. Modified frame error rate calculation

The 802.11s standard does not define a specific method to calculate the average frame error rate. As a specific implementation example, NS-3 simulator uses an exponentially weighted moving average, where the last known average frame error rate is weighted by a coefficient that decreases exponentially with time, and the result of the most recent transmission have more weight. One disadvantage of this method is that it depends on user data transmissions, and thus the measure is not accurate during idle periods.

In this paper, we propose an alternative method to measure the frame error rate on a link. Specifically, this involves sending *probe* packets between neighbors, and measuring how many of those packets have been received in the forward and reverse direction for each link during a given period. Nonetheless, there would be a drawback of increasing the network overhead when implementing this method which may be counter-productive in improving throughput.

Therefore, we need to come up with a method that does not add any overhead by avoiding the transmission of additional frames. To this end, we propose using information already sent by every node in the network through the use of *Beacon* frames, which are already part of IEEE 802.11s mechanisms. Specifically, this is possible via a protocol called *Peering Management Protocol (PMP)* [28].

Apart from HWMP, in 802.11s by default for path discovery and maintenance, PMP is other important protocol, which is responsible for neighbor mesh station (peer) discovery and link management. The PMP opens new links to neighbor stations and also closes links when failures on them are detected. Mesh stations are not allowed to transmit frames other than the ones used for peering management (Open/Confirm/Close) to a neighboring mesh station until a corresponding link has been established [28]. To make neighbors aware of its presence, every mesh station sends periodically small one-hop management frames, known as *beacons*. Each beacon broadcasts information about the station capabilities which includes supported rates, extended supported rates in addition to what is important for our purpose: the beacon timing containing the beacon interval and the time at which the reporting station last received a beacon from every neighbor. In this way, we will be able to compute average frame rates in forward and reverse directions.

Fig. 2 shows an example for this calculation with a network of 6 nodes and considering the link between nodes A and B specifically. Both *A* and *B* broadcasts beacon frames at a specific interval. By defining a window size and counting the number of beacons received during that time window, node *A* can get a frame delivery ratio from B to A. For instance, if the window size is set to receive 10 beacon intervals in the ideal case and 1 beacon is missed for whatever reason, then the frame delivery ratio in the forward direction (*B* to *A*) is $f_{df} = 9/10$. The same equation applies to calculate the frame delivery ratio in the reverse direction f_{dr}: Node A keeps a record of timestamps read from the beacons so that it can obtain a count of its beacons received by node B.

Consequently, putting these together, we can compute an extended bidirectional average frame error rate, ex_{fr}, as defined in Eq. (2) to be included in *SrFTime*, where f_{df} and f_{dr} are the frame delivery ratio in the forward and reverse direction respectively:

$$ex_{fr} = 1 - (f_{df} \times f_{dr}) \tag{2}$$

This is inspired from the approach of ETX computation. Basically, we multiply f_{df} and f_{dr} to compute average delivery ratio in both directions on the link and then we subtract it from 1 to come up with the error rate.

Table 2
SrFTime Metric Values for 802.11g.

Modulation	Default Airtime	Proposed SrFTime
Dsss1Mbps	887	217
Dsss2Mbps	470	165
Dsss5_5Mbps	205	117
Dsss11Mbps	130	96
ErpOfdm6Mbps	177	110
ErpOfdm9Mbps	131	96
ErpOfdm12Mbps	108	88
ErpOfdm18Mbps	84	79
ErpOfdm24Mbps	73	73
ErpOfdm36Mbps	61	67
ErpOfdm48Mbps	55	63
ErpOfdm54Mbps	53	62

4.3. Link time usage calculation

The second modification to the default airtime link metric calculation is related to the airtime portion specifically. We would like to motivate this modification with a concrete example. According to Eq. (1), the default airtime metric for a 1Mbps link with no errors is 887, and 470 for 2Mbps. Next, let us assume that the 2Mbps has a average frame error rate of 46%, the resulting metric is now $470/(1-0.46) = 870$. If one mesh station has two possible paths to follow, it could still prioritize the 2Mbps link over the 1Mbps link ($870 < 887$) even if the first one has a frame error rate of near 50%.

Our approach for the new metric allows more contribution from the error rate component by eliminating the direct proportionality between time in the air (B_t/r) and the final metric value, where α and β are weighting factors as shown in Eq. (3).

$$SrFTime = \left(\alpha O + \beta\sqrt{\frac{B_t}{r}}\right) \times \frac{1}{1 - ex_{fr}} \tag{3}$$

Basically, we propose to get square root of B_t/r to reduce its impact on the overall metric. Moreover, we tuned the values of α and β in our implementation. After comparing the results of several experiments, it was determined that $\alpha = 1$ and $\beta = 20$ provide a sustained improved performance. We maintain the requirement to have the final metric divided by 0.01 TU (Time Units) or 10.24μ; *s* as per the standard. The new metric values for different link rates and zero frame error rate are shown in Table 2. As seen, we were able to reduce the values of Airtime metric, which will eventually impact the routing decisions for improved throughput.

5. Routing metric optimization for mobility

SrFTime metric aimed at improving network throughput when the nodes are stationary. However, as mentioned earlier FANETs may exhibit high mobility depending on the applications, which causes an increase in the number of link changes. For instance, some links may be broken eventually due to movements while new links are established. Therefore, in order to improve the network performance, it is imperative to account for variations in the links caused by the change of relative positions between nodes and incorporate those indicators into the link metric.

A potential intuitive approach to account for mobility effects in the metric is to use the relative location and velocity of neighboring nodes through GPS. Since drones have built-in GPS used for location and flight control, a drone's location and velocity could be shared with neighboring drones to calculate how far they are from each other and estimate their relative position after a brief period of time. Nonetheless, physical location by itself cannot be used to determine with good precision when a link is about to be broken because a given transmission (Tx) power and link distance will produce a different reception (Rx) Power at the receiver node depending on many factors. These factors include but not limited to the type of environment (rural, urban, etc.), and the nature of obstacles and weather/atmospheric conditions blocking Line-of-Sight (LoS) capabilities. Therefore, we opt to rely on Rx power as a more reliable indicator to accommodate mobility effects.

Specifically, when two nodes get far from each other, the attenuation of the radio signal that travels between them increases, resulting in less Rx Power. The consequences of a reduced Rx Power include reduced signal to noise ratio (SNR) and link breakage if Rx Power drops below the receiver sensitivity level also known as Energy Detection Threshold (Ed_T). In our case, because of the high mobility of drones, it is possible that two nodes that are communicating just fine could suddenly lose connection because of loss of signal (i.e., Rx power drops below Ed_T). While mobility may not be the sole reason for this, it is the main cause and it needs to be accounted for both sides considering that in a mobile mesh network all nodes are typically configured with the same transmission power.

Based on these observations, our revised metric utilizes the Receive Signal Strength Indicator (RSSI) which is the power level of the received frame as a more accurate method to determine when a node is nearing the transmission coverage limit.

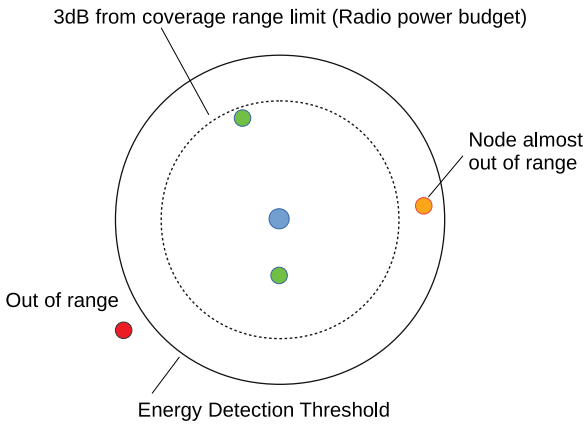

Fig. 3. Node coverage range and warning zone.

Therefore, we modify the SrFTime link metric further by adding a new component that will increase the metric value when the RSSI value is so close to Ed_T as an indicator that a link break is very likely to occur. Furthermore, we note that we do not increase the link metric when RSSI value is within normal values. In other words, when the nodes are within good range from each other as determined by RSSI, we let the best route to be chosen by SrFTime metric, and only when the nodes are close to the transmission coverage boundaries inside a 'warning zone', we would like to increase the link metric so that the nodes considering this transit link eventually selects a more suitable one assuming there are alternatives before a link break occurs. This is depicted in Fig. 3 where we show a reference node as a blue circle and its four neighboring nodes. The orange neighbor is located in the warning zone which we define as the zone within k dB from the coverage limit where k could be set experimentally. For nodes in that region, we strive to increase the value of the link metric (i.e., the link will not be picked by the routing algorithm) as it is prone to be out of range at any moment.

Putting it all together, we can add this enhancement due to mobility to our SrFTime metric which is called Comprehensive Radio and Power (CRP) metric hereafter. CRP basically aims to take into consideration the likeliness of a link break when there is a small margin between the Rx power and the Energy Detection Threshold Ed_T as stated in Eq. (4):

$$CRP = \begin{cases} SrFT + \gamma\left(10^{\frac{k-PB}{10}} - 1\right) \times \frac{1}{1-ex_{fr}} & \text{if } PB < k \\ SrFT & \text{otherwise,} \end{cases} \tag{4}$$

where γ is a weighting constant and PB is the power budget in dB defined by:

$$PB = RSSI - Ed_T \tag{5}$$

Note that Ed_T is a value configured in the network device and it is available to use. The determination of the optimum k threshold is based on experiments. By evaluating different values and picking the threshold that resulted in better performance we came up with a k threshold of 3dB.

6. Complexity analysis

In this section, we analyze the complexity of the proposed routing metric for FANETs in terms of its computational and communication complexity. Computational complexity is important from the perspective of drone's resources as a drone might not have a lot of CPU and memory resources. Communication complexity, on the other hand, is crucial in understanding the performance of routing protocol when the network scales. Note that we only consider the metric for the mobile cases as it already supersedes *SrFtime* metric for the stationary cases. In other words, the complexity of *CRP* is either same or a little worse than *SrFtime*.

6.1. Computational complexity

The computations in our proposed *CRP* metric utilizes existing information such as RSSI values to perform constant number of arithmetic operations and thus their cost in the worst case is still constant: $O(1)$.

6.2. Communication complexity

The number of communications needed for gathering the information for computations for a node is our measure for node complexity. In our approach, we do not introduce extra messaging to collect RSSI or other information. These are coming from beacons which are broadcast periodically as part of the IEEE 802.11s meshing standard. However, we can still

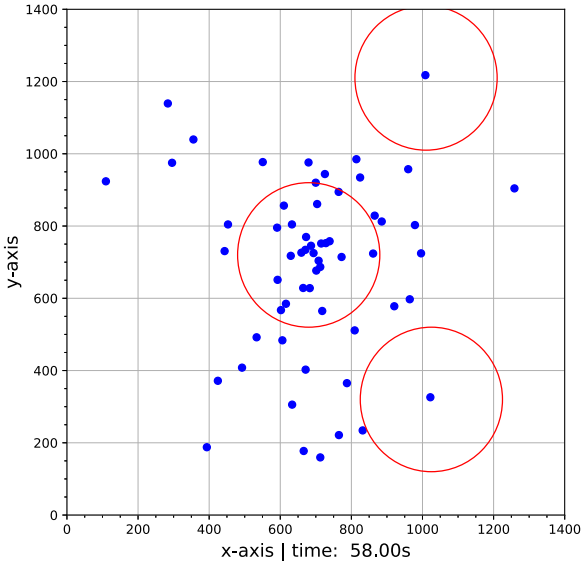

Fig. 4. RPGM scenario with 60 nodes using BonnMotion.

count these messages to reflect an overhead. Basically, each node sends 1 broadcast beacon while it will receive k broadcast beacons from its neighbors where k is its neighbor count. This means for a node there will be a total of $k+1$ messages and thus the communication complexity will be $O(k)$ per node. Note that even though the total number of drones, n, is increased our communication complexity will still be constant since typically the average number of neighbors for a node in a network would not change much.

7. Mobility model for FANETs

While it is important to customize a routing metric for FANET applications, it is also crucial to come up with realistic mobility models for FANETs that can be utilized in simulation-based testings since often actual deployment and testing of FANET research is very difficult. This need is also evident in the current research since most of the published research work on FANET performance experimentation considers trivial mobility models [24] that fail to represent a realistic formation and movement pattern of a swarm of drones. This is because traditional mobility models are purely random-based and does not exhibit such characteristics. Currently, there is no mobility scenario that has a strong correlation with the real mobility of a swarm of drones in 3-D environments. In addition, the work in [33] reports that "the flight characteristics of UAVs in 3-D environment have been neglected, leading to inaccurate experimental results".

Consequently, the simulation of FANET node movements requires to use an appropriate mobility model that better represents the pattern and cinematic characteristics of drones, thus allowing to obtain more accurate results compared to other existing mobility models. In particular, since swarm of drones are used because of the many advantages they provide when performing cooperative tasks, their mobility should exhibit smooth changes in speed and direction, as well as group synchronization and [24] mechanisms for collision avoidance.

We claim that the best fitting mobility models for swarm of drones would be group mobility models [34]. Although there have been some group mobility scenarios proposed to be used for drones, they still need some adjustments to mimic the movements of an efficient 3-D mobile network. This is mostly due to the fact that the movement patterns in a swarm would follow a mixture of individual and group-based needs. In addition to this issues, there are difficulties with the implementation and availability of the proposed group models whether it is geared for drones or other applications. In most of the cases the corresponding scenario generator was - to the best of our knowledge - not published or available to use.

To this end, we picked the RPGM model for adaptation to FANETs. As introduced in Background Section, RPGM allows us to define groups which can have their own mobility patterns and in each group there is a reference point. In addition, RPGM models could be generated by a mobility generator tool called BonnMotion [35,36] which is available to use. However, RPGM had two problems when it comes to FANET adaptation. First, BonnMotion's RPGM was designed for 2-D MANET simulation rather than for 3-D scenarios. Second, in RPGM large size groups exhibit non-uniform distribution of nodes as depicted in Fig. 4. It can be observed in this figure clearly that the center of the area have a higher density of nodes and some of these nodes even get dangerously close to other nodes. In contrast, the nodes located far from the group center have a more sparse distribution, potentially isolated and disconnected from the swarm.

To adapt this model for FANET environments, a post-processing of the scenarios generated was required as follows:

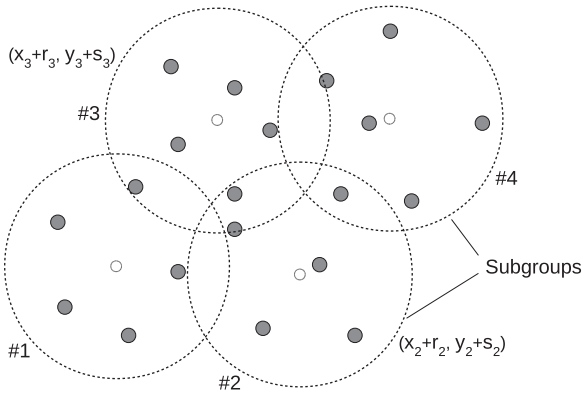

Fig. 5. Group Mobility Scenario by merging RPGM subgroups. White circles are the reference points for the subgroups.

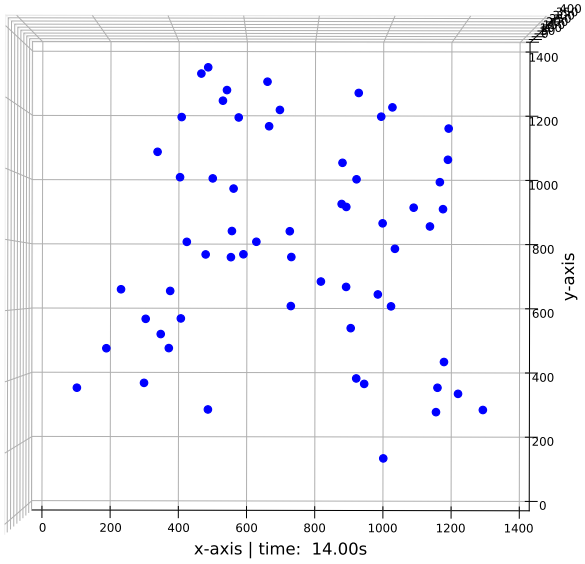

Fig. 6. Upper view of 3-D proposed group mobility scenario.

- To create subgroups with a manageable number of nodes, so that dense distribution of several nodes is minimized and potentially isolated nodes are eliminated with the goal of obtaining more uniform node distributions.
- For each subgroup, linearly scaling each node's Z-coordinates to a suitable range for swarm-of-drones.
- Move each (x_i, y_i) within a subgroup i to a new location $(x_i + r_i, y_i + s_i)$ so that when placed in a common 3-D system they become adjacent groups with appropriate separation among each other. Here, r_i, s_i are the displacement values based on the actual distribution of nodes in subgroup i relative to the nodes in the common 3-D system.
- To merge all different subgroups into a single swarm. This is done by bringing all subgroups movement information into a single file in BonnMotion's format.

Fig. 5 illustrates this process using an example of a 20-node mobility scenario created from 4 RPGM-subgroups with 5 nodes each. Note that when RPGM-subgroups are created, some nodes may be discarded to avoid extreme low or high density of nodes. Therefore, at the time of creation, the number of nodes per subgroup is chosen slightly higher than the desired number of nodes so that we can discard the ones that tend to deviate more from a cooperative group formation.

To compare with the topology in Fig. 4, we generated a new topology using our proposed mobility model as shown in Fig. 6 where we combined 6 RPGM-subgroups with 10 nodes each for a total of 60 nodes. We can observe how following the approach of sub-group merging ensures a better distribution of nodes. There can still be nodes that at some point in the simulation move close to other nodes, but the agglomeration is a lot less. Hence, it allows a more cooperative efficient network overall. Fig. 7 shows the 3-D view of the same topology with 60 nodes.

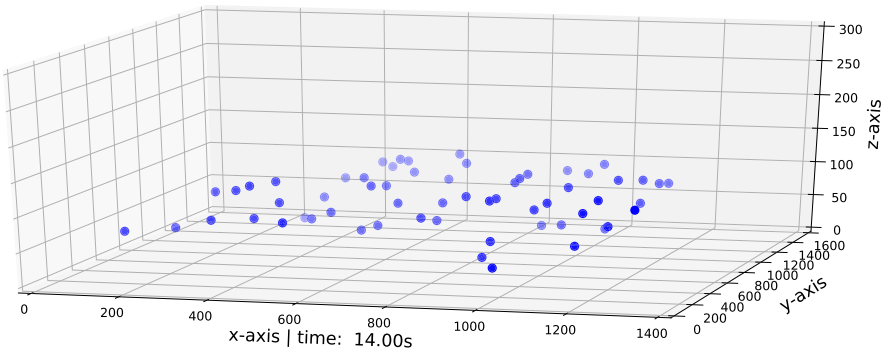

Fig. 7. Example scenario using proposed 3-D mobility model.

Table 3
NS-3 simulation network and test parameters.

Parameter	Set to
Network Simulator	NS-3 (v3.29)
RemoteStaManager	MinstrelHt
Wifi Standard	802.11n 2.4 GHz
Max. Spatial Streams	1
Radio Frequency	2.437 GHz
E. Detection Threshold	-87 dBm
Traffic Pattern	Constant Bit Rate
Packet Size	536 bytes
Number of Nodes	60
Z Coordinate Range	30–120m
Propagation Loss Model	Friis, ITU-R1411
Stationary Data Traffic Time	100s
Stationary Simulation Area	(2400 × 1200) m^2
Mobile Data Traffic Time	120s
Mobility Model	Proposed Custom RPGM

8. Performance evaluation

8.1. Simulation setup

To determine and quantify the performance improvement of the proposed metrics, we implemented them within IEEE 802.11s module in NS-3 v3.29 [37] network simulator. We followed a cross-layer approach in our implementation to retrieve information about Energy Detection Threshold and about RSSI through tagging.

We created random FANET topologies of size 60 to be used during the simulation. In these topologies, each station sends data at a constant bit rate to the root node, which is selected among the drones with the highest altitude in the swarm considering that this will be a gateway to another network in a complete real scenario. All parameters configured in NS-3 are shown in Table 3.

We considered experiments for stationary (i.e., hoovering drones) and mobile drones separately and thus their setup was also different as explained below:

8.1.1. Stationary nodes

The station's locations were selected randomly, representing a group of drones located inside an imaginary cube with dimensions 2400 × 1200 × 120m. All stations are configured with the same Tx Power Level depending on the propagation loss model (0dbm for Friis and -4dBm for ITU-R1411). Therefore, the topologies were adjusted so that there is a minimum distance between any two stations and also no station can be separated from the group for more than a maximum defined distance. Two sets of scenarios with different distance constraints were generated, one set with 100m/250m min/max and another set with 120m/230m. Each set with 30 different topologies add up to a total of 60 topologies or scenarios. Also, the minimum height for any station was set to 30m (the Z coordinate range selection makes a difference when using ITU-R1411 as the propagation loss model). The results provided correspond to the average of running the simulation tests over all 60 topologies to achieve statistical significance.

8.1.2. Mobile nodes

In case of mobile topologies, we used five 3-D scenarios with a Z-coordinate range of 30m to 120m. This range is picked since some drones capture image or video from the terrain at lower heights while the upper nodes can be used to relay

the communication. For generating drone locations randomly, we had some challenges. This is because the minimum and maximum distance between nodes cannot be easily controlled in RPGM and if the topology creation is not controlled, we may end up with topologies that either do not have any routes to the gateway node or experience too much collision due to proximity of the nodes [25]. Therefore, each topology was tested using at least 3 different Tx power values and we chose for each topology the results that produced the highest throughput collectively (i.e. for all routing metrics). By using the optimal Tx power, we ensure that in general nodes will have enough links to choose from when finding a path to the destination and thus allowing the conditions to better evaluate the performance of the routing metrics. The simulations tests are performed as in the case of stationary nodes where 59 mobile nodes are sending data to the root node. The results presented are the average of the results from all mobile scenarios.

8.2. Mobility model implementation

For implementing the proposed mobility model adapted from RPGM, we used *Ns2MobilityHelper* class in NS-3 as a helper to import NS-2 (i.e., former version of NS-3) movement trace files for simulation into NS-3. Its use is very convenient as an alternative to the mobility models built in NS-3. Third party applications that generate mobility scenarios could export the location and mobility information in a compatible format that can be ported to other network simulators.

However, NS-2 movements were conceived for 2-D networks. This limitation is a hurdle for effective simulation in 3-D FANET that we needed to overcome.

Therefore, the Ns2MobilityHelper files were upgraded to allow scenarios with full 3-D mobility. As such, the following statement can now be parsed by the enhanced Ns2MobilityHelper class:

```
$ns at $time $node setdest x2 y2 z2 speed
```

With this improvement, suitable mobility scenarios for FANET simulation could be imported for simulation into NS-3, and the updated files are freely available to use [38]. As part of this work, we also developed a tool to convert 3-D mobility scenarios from BonnMotion format to NS2 mobility trace files format [39].

8.3. Metrics and baselines

The main metrics we used for assessing the performance are listed below:

- *Network throughput* which is determined by calculating the total data received by the root (gateway) node and dividing it by the time the nodes send the data.
- *End-to-end delay* which is computed by averaging all the end-to-end delay of the packets sent from every node in the network to the gateway node.
- *Route Changes* which indicates the number of route changes for all the nodes as an indicator of overhead. A route change is considered a change in the route table entry for packets destined to the root node.

For comparison, we used the default *Airtime* metric as the baseline. To validate the results under different scenarios and network variables, simulations were run considering both TCP and UDP as well as two propagation loss models: Friis and ITU-R1411 LOS. Basically, Friis is just a baseline but ITU-R1411 LOS realistically reflects the path loss in FANET environments and its results will be crucial. As mentioned, we tuned the initial TX power for the nodes for each of these models to obtain an adequately connected network what will provide routes from each node to the gateway node.

8.4. Simulation results

We conducted experiments for both stationary and mobile topologies to see the impact. In this subsection, we first report results of stationary topologies and then move to mobile topology results.

8.4.1. Throughput results - stationary

We first conducted experiments to see the impact of the proposed metrics on throughput. In these experiments, we varied the data rate (5/10/20/40kbps) from each drone for UDP and TCP traffic. We also collected results under different propagation loss models. The results are shown in Fig. 8.

We observed that under the Friis model, the network throughput increases about 26% in average consistently when *SrFtime* metric is used in routing of TCP traffic and about 14% for UDP traffic. The improvements follow a similar pattern for *CRP*, slightly behind the *SRFTime* metric. Similarly, under the ITU-R1411 model, we observe that our metrics still performs much better (i.e., about 12% for TCP and 10% for UDP) though it is not as much as in the Friis model. These significant improvements can be explained by the route changes with the proposed metrics. We observed that the number of route changes in the network is reduced about 17% in average when *SrFTime* and *CRP* are used as compared to *Airtime* as shown in Fig 9. Specifically, it is known that some metrics suffer from self-interference [40], causing a negative effect in network performance. For the proposed metrics, the routes are therefore more stable which work in favor of increasing the network throughput.

When comparing *CRP* to the *SrFTime*, we observe that the latter is slightly better. This indicates that in general for stationary networks the longest links are important to have an efficient wireless network. By penalizing the longest links with

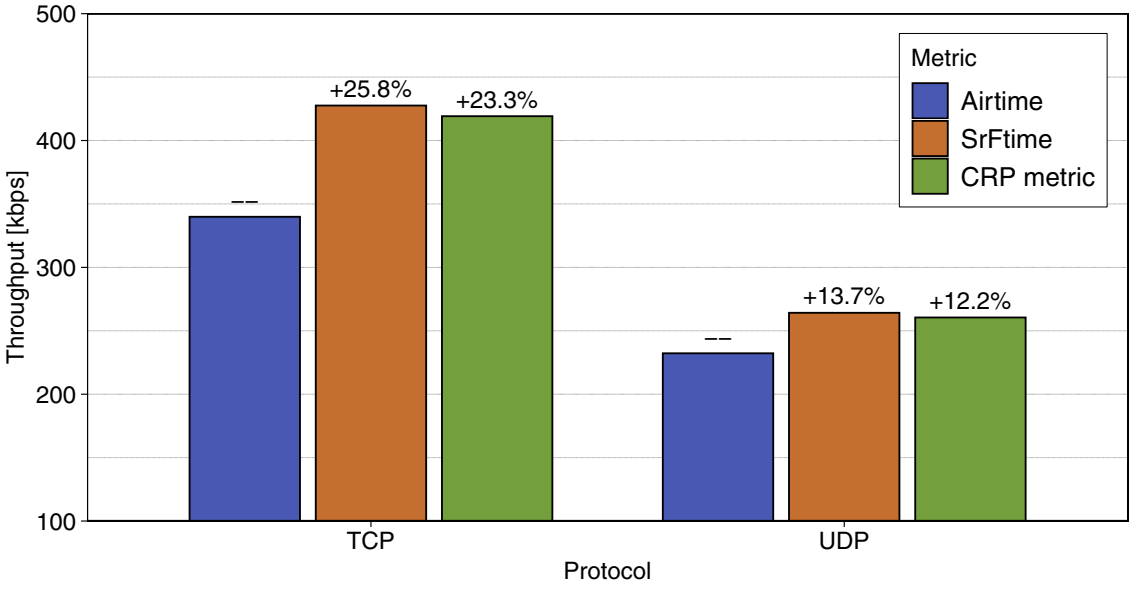

(a) Friis Propagation Loss Model

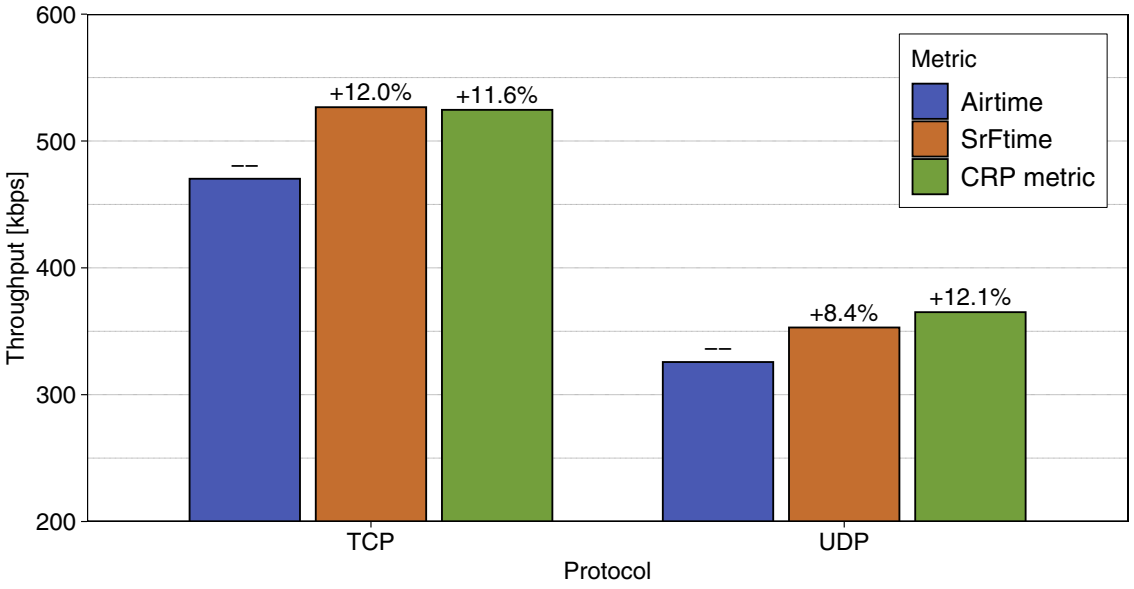

(b) ITU-R1411 Propagation Loss Model

Fig. 8. Network throughput - stationary FANET.

an additional component and forcing the routing protocol to avoid them when possible, we are decreasing the throughout slightly in the *CRP* case.

The other interesting observation is that the percentage in average network throughput improvement is higher for TCP compared to that of UDP. This might be attributed to the ways these protocols are designed. In case of TCP, when there is a route failure, there needs to be a re-transmission to enable reliability. In case of our metric, paths with higher reliability are chosen, which results in less re-transmission. However, this is not the case for airtime metric where path reliability might be less. Re-transmissions cause a lot of overhead and may interfere with other ongoing transmissions causing more

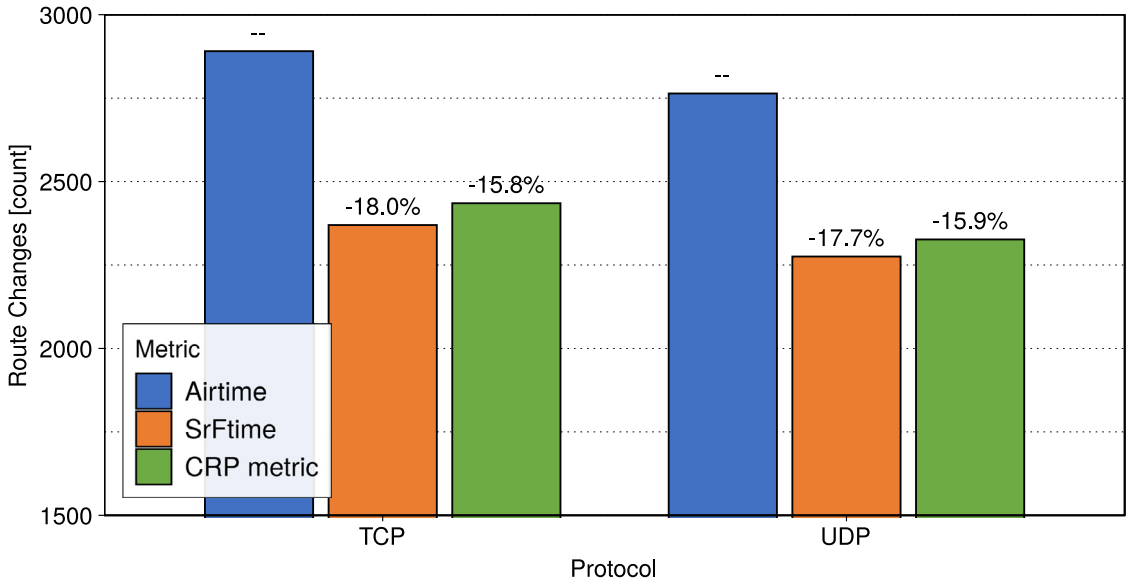

(a) Friis Propagation Loss Model

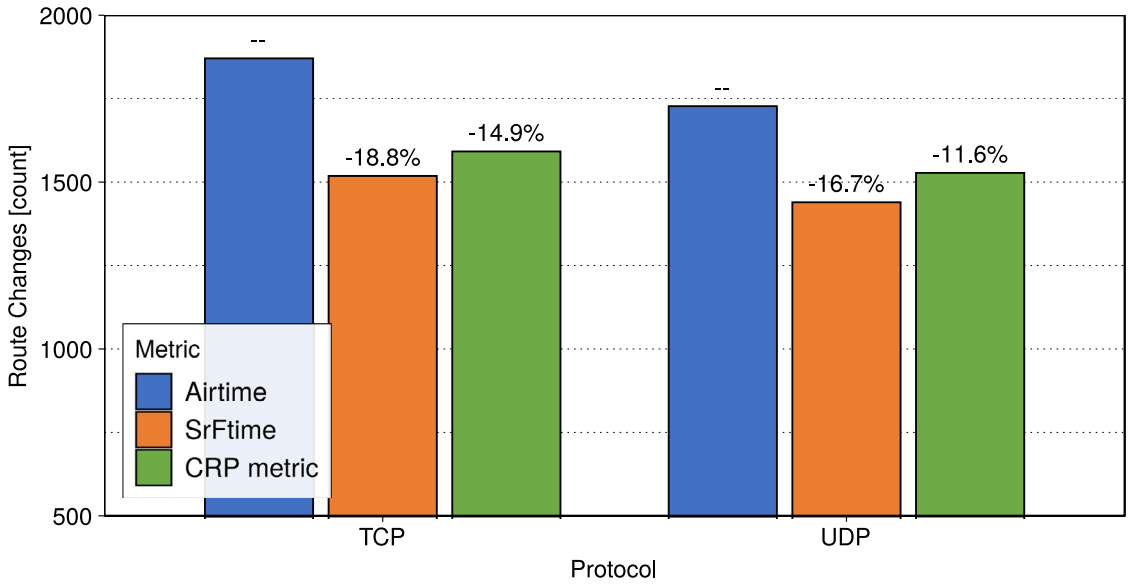

(b) ITU-R1411 Propagation Loss Model

Fig. 9. Number of route changes - stationary FANET.

packet losses. Therefore, any improvement in this process will automatically benefit the throughput significantly. In case of UDP, this is not an issue. If there is a failure, there is no re-transmission effort and thus interference with other route transmissions is not possible. Therefore, the impact of the new routing metrics on this protocol will be comparably lower.

Finally, comparing the behavior under different propagation models, we see that ITU-R1411 does not benefit from the proposed metrics as much as the Friis model when TCP is considered. We speculate that this might be due to the way these models work. Friis propagation loss model is a simple model in the sense that the only geographical input it takes is the separation between nodes while ITU-R1411 also takes into consideration the height from the ground to calculate the

propagation loss. Lower stations experience more attenuation than the ones located at a higher altitude which might be overall benefiting percentage of improvement in Friis more due to all nodes being treated in the same manner.

8.4.2. End-to-end delay results - stationary

We next assessed the impact of our proposed metrics on average packet delay. This was needed as increased throughput might increase traffic and hence cause delay.

The results shown in Fig. 10 indicate that *SrFTime* also positively contributes to end-to-end delay for both propagation loss models. Specifically, it reduces significantly the overall delay when UDP is used. For TCP, *SrFTime* performs similar to the *Airtime* metric and the trade-off introduced is minimum. The reason behind the delay reduction for UDP could be due to the fact that the proposed metric finds better routes and thus reduces packet delays. In the case of TCP however, this is not apparent as the increased quality in the path only increases reliability and thus throughput but this comes with more overhead in delay or perhaps longer paths which eventually slightly increases delays overall.

The slight decrease in the performance of *CRP* with respect to *SrFTime* follows from the behavior explained when analyzing the throughput performance. By influencing the link metric so that the routing protocol avoids the links very close to the coverage limit, we pick the links with medium and shorter distances with *CRP*. Thus, this may potentially increase the number of hops and thus the end-to-end delay. These results are expected since stationary nodes will not have broken links for out-of-range mobility issues.

Comparing the different models, the impact on ITU-R1411 is a bit less. Especially for UDP, *Airtime* already provides less delay and thus there is less room for improvement.

8.4.3. Throughput results - mobile scenarios

In the second part of the simulation experiments, we evaluated the performance of the proposed metrics under mobile topologies. As mentioned, our proposed mobility model has been used in these experiments. The results correspond to the average of testing at different station data rates 5/10/20/40 kbps and across five mobility scenarios.

Based on simulations, we found that the selection of the most optimal weighting coefficient γ for *CRP* metric defined in Eq. (4) varies when using different propagation loss models. When using Friis propagation loss model, it was determined that $\gamma = 30$ provides a sustained improvement when applied to the different mobility scenarios. Similarly when $\gamma = 54$, this metric performs better when ITU-R1411 is used. A reason for this is that the 3dB margin considered in that metric can be translated to different distances for different propagation loss models. Then by adjusting the coefficient γ, we can account for those differences and optimize the metric.The results for throughput are shown in Fig. 11.

As seen in the figure, *CRP* metric provides a remarkable increase of over 32% in network throughput compared to *Airtime* for TCP traffic under both propagation loss models. Even for UDP traffic, the improvement is still significant compared to stationary case: 12% when using Friis and 24% when using ITU-R1411 propagation loss model. *SrFTime* still outperforms *Airtime* (i.e., around 20%) but is definitely not as effective as the *CRP* metric. As in the stationary experiments, the number of route changes for both metrics is always less than that of *Airtime* metrics in any case as seen in Fig. 12. We observe that there is slight reduction in *CRP* metric route changes compared to *SrFTime* (which is contrary to stationary case) and thus this helps keeping routes more stable with *CRP* metric, helping to improve the throughput.

In addition to route stability, these performance measurements corroborate the logic behind the metric definition: making nodes reconsider an alternate next hop node when the current node is very likely to be off-range thus resulting in a link break and a subsequent re-transmission of TCP packets, proves to be advantageous. When an alternate route is chosen before a link break occurs, a smooth route update takes place, reducing the negative effects of having a link break such as increased buffering and re-transmissions. In the case of UDP there is no re-transmissions, therefore the improvement is slight which can be attributed to reducing the number of packets that would have been lost should an alternate route not be chosen before a link break occurs.

These results also show another interesting trend: Under ITU-R1141 model, *CRP* metric improvement is much better. This was not the case for Friis model. This shows that our metric would be very suitable to be implemented in real environments.

Overall, we can argue that our approach to metric optimization does not aim to counter completely the negative effects of link breaks, but rather provides an overall improvement without increasing the network overhead that occurs when additional probe or control packets are sent.

8.4.4. End-to-end delay results - mobile scenarios

Next, we analyzed the impact of using our proposed metrics on end-to-end delay under the mobility scenario. The results are shown in Fig. 13. From these results, we observe that the results for both *SrFTime* and *CRP* metrics related to *Airtime* for UDP are similar to those obtained in stationary networks and thus there is no impact on delay. When considering the delay under TCP, the results are even better than the stationary case for both metrics. There is reduction in case of *SrFTime* metric while the amount of increase for *CRP* metric is slightly less. It is also interesting that the delay is not impacted from propagation models, again predicting the practicality of our metrics in real deployments. Overall, there is negligible impact on delay for both metrics under any conditions, indicating the promise for our metrics.

8.4.5. Scalability analysis

In this part of the experiment, we analyzed the scalability of our routing metric by comparing the throughput results for two different mesh network sizes. We basically tripled the network size to see its impact on performance.

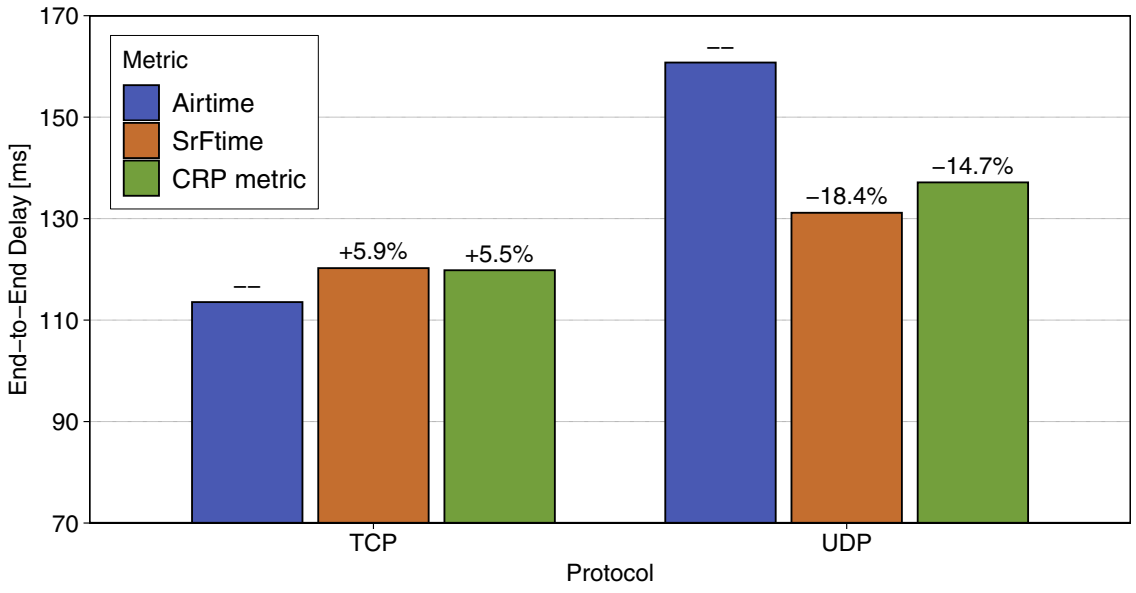

(a) Friis Propagation Loss Model

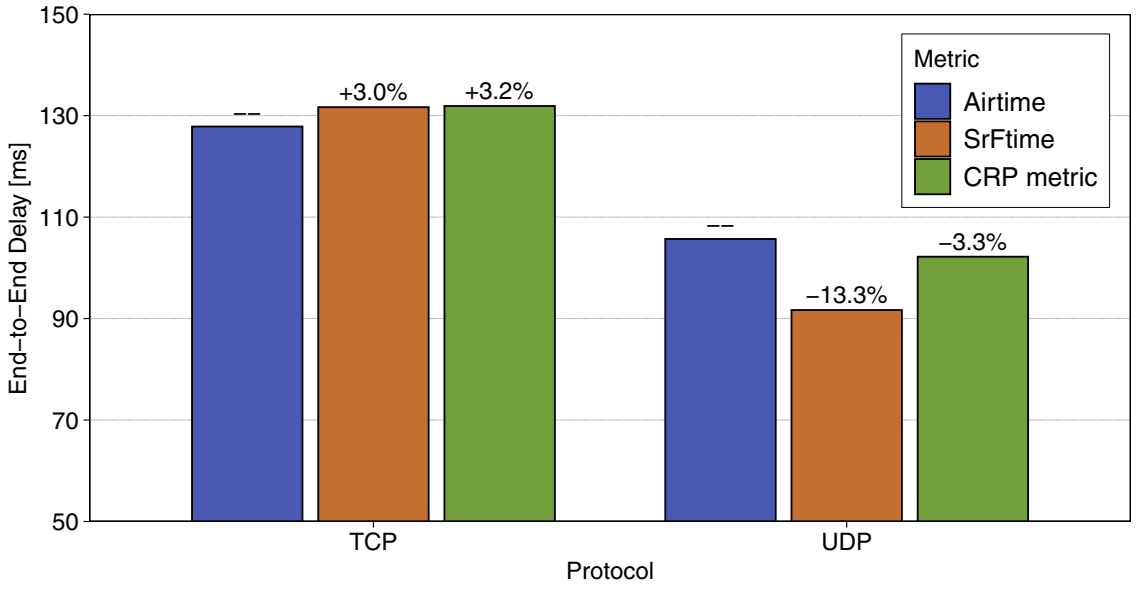

(b) ITU-R1411 Propagation Loss Model

Fig. 10. End-to-end delay - stationary FANET.

We ran experiments using five (5) mobile scenarios with 20 nodes for a single propagation loss model and data rate (Friis/10 kbps respectively) and compared the results with the corresponding results for mobile scenarios with 60-nodes. Fig. 14 shows that from the three metrics compared, *CRP* shows the most stable performance maintaining the network throughput while increasing the number of nodes, followed by *SrFtime* and then *Airtime*. We see that *CRP* is able to sustain the performance as its results are stable. This is the only metric that shows promise in terms of scalability. As the number of nodes grows, there is a lot of congestion in the network due to increased number of transmissions and channel access requests. This naturally reduces the throughput but on the other hand there is more data generated from more nodes.

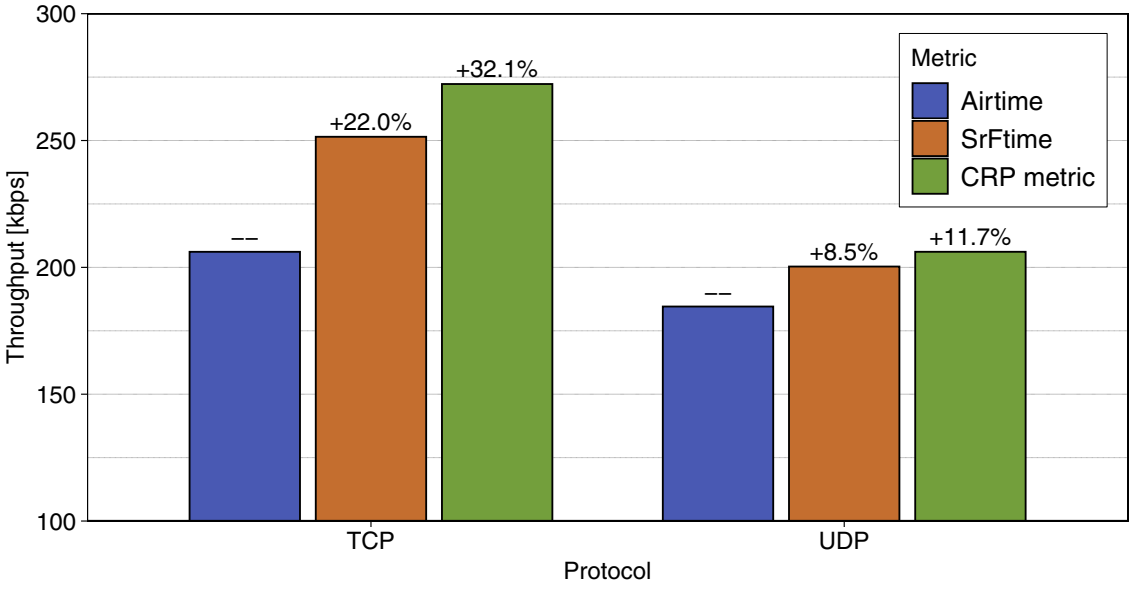

(a) Friis Propagation Loss Model

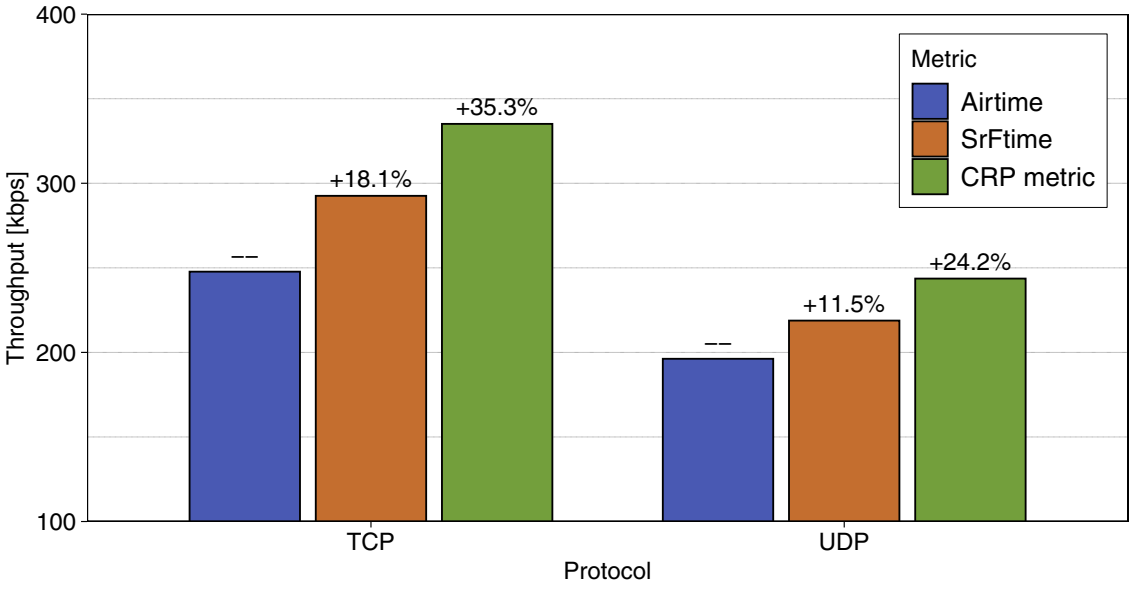

(b) ITU-R1411 Propagation Loss Model

Fig. 11. Network throughput under mobility.

Therefore, we should be able to keep the throughput stable and this is possible with *CRP*. It is interesting to note that for a mesh network of 20 nodes, all three metrics perform very similar. This is because, there is less interference between nodes and the network can manage to deliver the data from every node whatever path is chosen by the routing protocol and the routing metric.

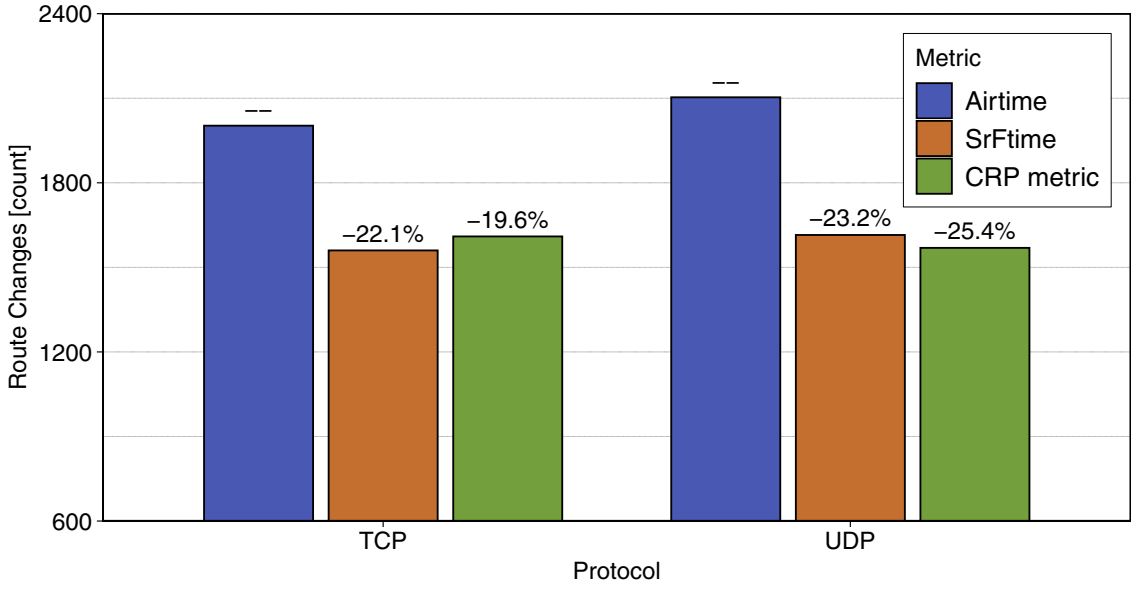

(a) Friis Propagation Loss Model

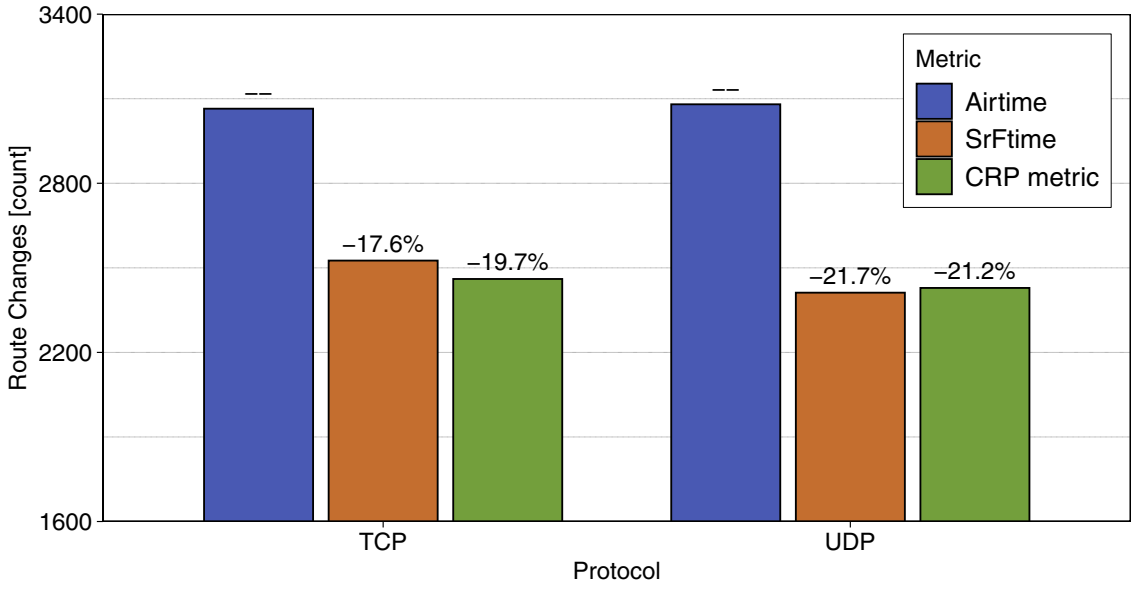

(b) ITU-R1411 Propagation Loss Model

Fig. 12. Number of route changes under mobility.

8.4.6. Comparison with AODV routing protocol

Finally, we wanted to compare HWMP with this new routing metric against the widely used AODV standard. This is just to verify that the new routing protocol with the new routing metric does improve the overall performance compared to existing state of the art. For our specific system model, we chose one mobile scenario and propagation loss model and compared the throughput results of the network using Mesh 802.11s standard with HWMP and the same network changing only the routing protocol for AODV. All other WiFi specific parameters were configured the same.

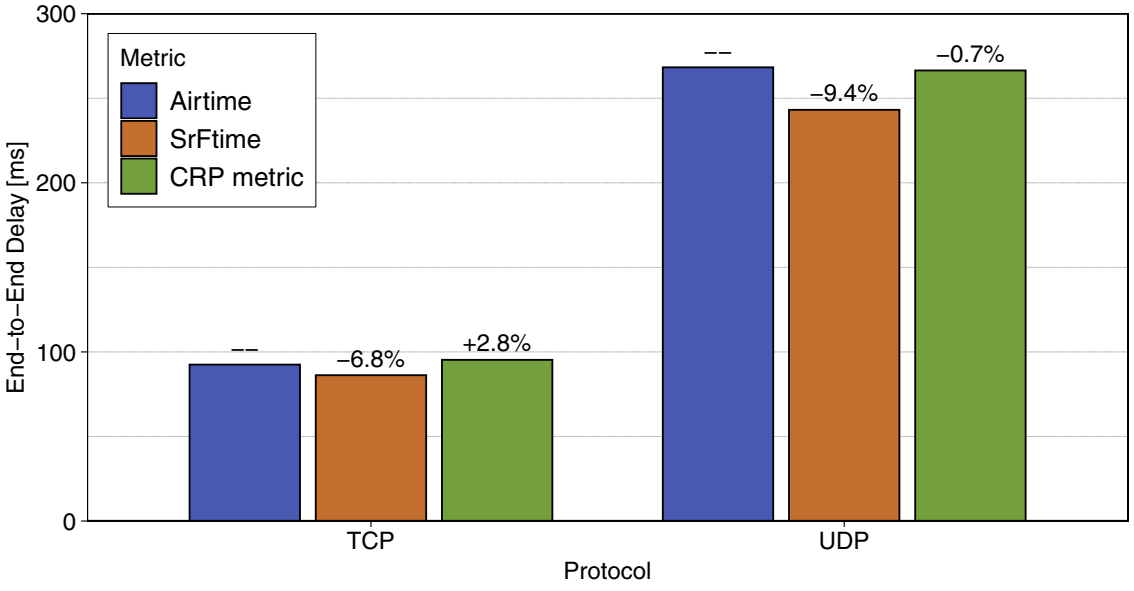

(a) Friis Propagation Loss Model

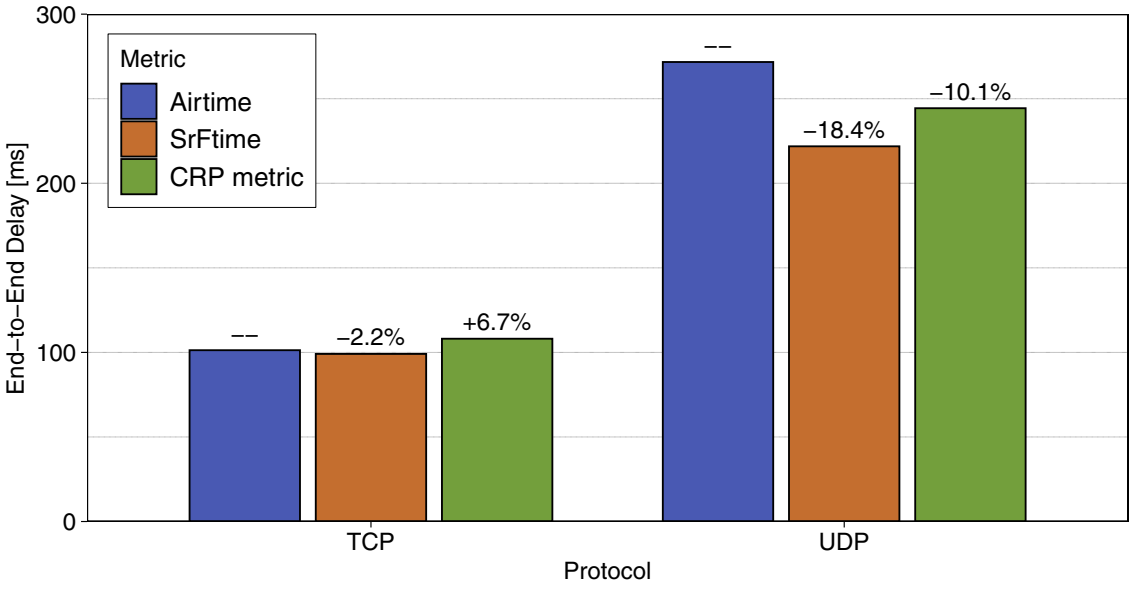

(b) ITU-R1411 Propagation Loss Model

Fig. 13. End-to-end delay under mobility.

Fig. 15 shows that for this sample scenario and physical parameters, the network throughput when using the HWMP with *CRP* approximately doubles compared to using AODV with hop count metric. These results indicate that our metric indeed help improve the current state of the art significantly.

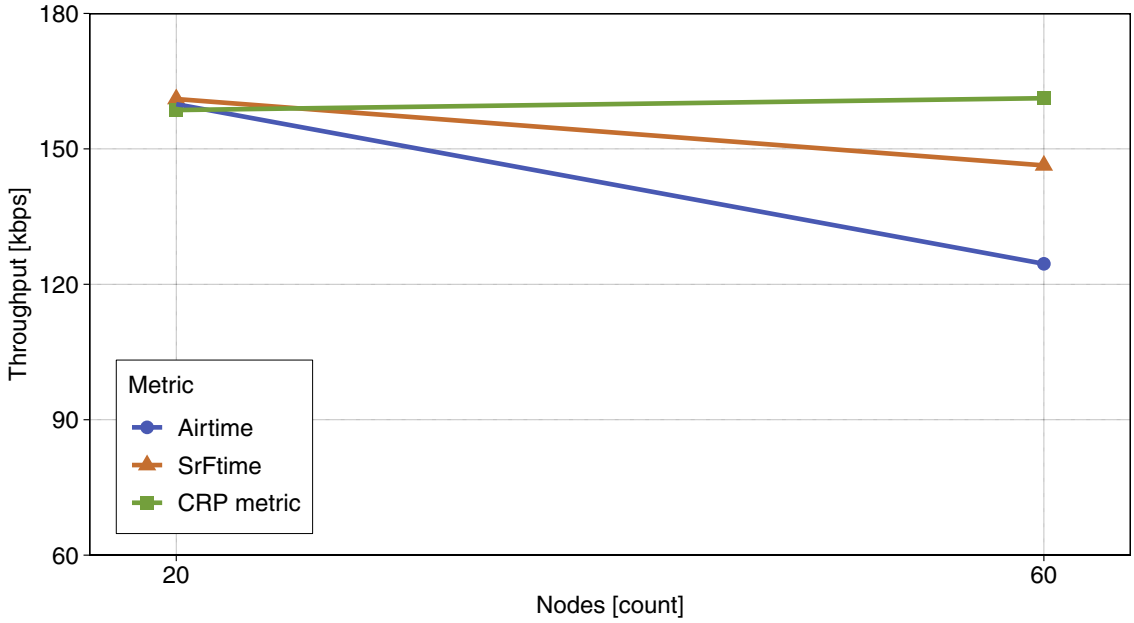

Fig. 14. Network throughput for different swarm sizes.

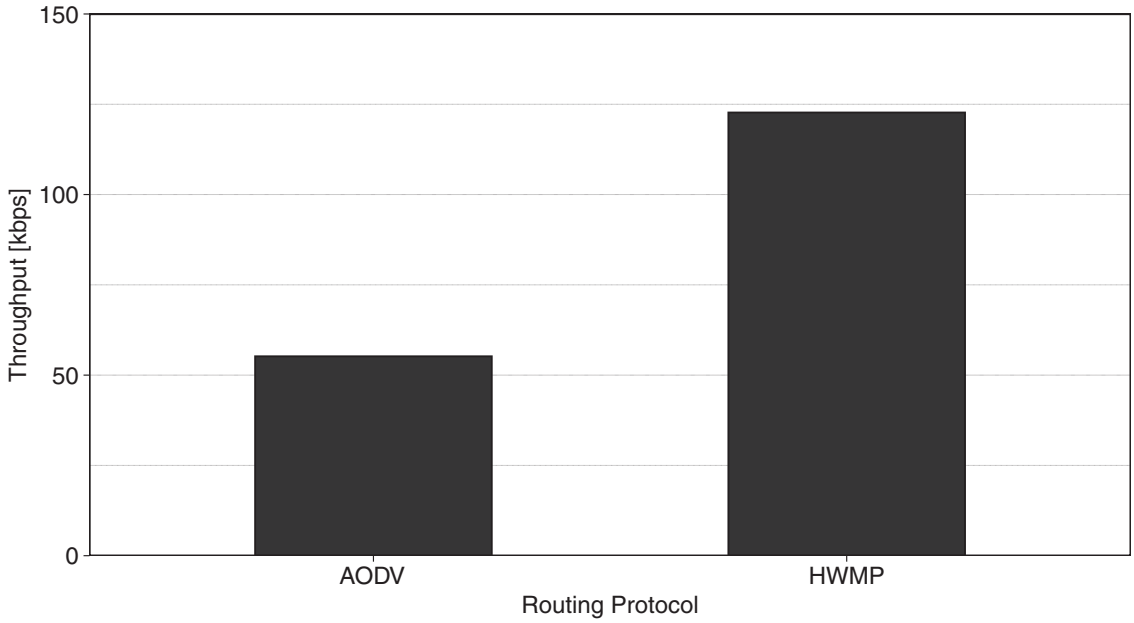

Fig. 15. Comparison between AODV and 802.11s's HWMP.

9. Conclusion and future works

In this paper, we targeted the current standard used for multi-hop communication among FANETs and aimed to improve the network performance through modifying the *Airtime* routing metric of 802.11s standard based on the needs of drone applications, avoiding to increase network overhead by using information available at each node. The new metric included more contribution from the error rates that might fluctuate due to changing environment of drones and their mobility.

Based on the simulation results, we show that the proposed *CRP* metric provides the best performance in terms of network throughput and can serve the needs of mobile FANETs or swarm-of-drones. *SrFTime* on the other hand is more suited for stationary FANETs which provides a balance between network throughput and end-to-end delay.

The source code containing the expanded model including both novel routing metrics is freely available for the research community to use [41].

In the future, we plan to explore the possibility of improving the performance by having the routing table store an alternate path which will be ready to be used when the preferred path is broken.

Declaration of Competing Interest

The authors declare that they have no known competing financial interests or personal relationships that could have appeared to influence the work reported in this paper.

Acknowledgment

This publication was made possible by NPRP grant #NPRP9-257-1-056 from the Qatar National Research Fund (a member of Qatar Foundation). The statements made herein are solely the responsibility of the authors.

References

[1] İ. Bekmezci, O.K. Sahingoz, ß. Temel, Flying ad-hoc networks (fanets): a survey, Ad Hoc Netw. 11 (3) (2013) 1254–1270, doi:10.1016/j.adhoc.2012.12.004.
[2] S. Hayat, E. Yanmaz, R. Muzaffar, Survey on unmanned aerial vehicle networks for civil applications: a communications viewpoint, IEEE Commun. Surv. Tut. 18 (4) (2016) 2624–2661, doi:10.1109/COMST.2016.2560343.
[3] G. Mohandas, S. Silas, S. Sam, Survey on routing protocols on mobile adhoc networks, in: 2013 International Mutli-Conference on Automation, Computing, Communication, Control and Compressed Sensing (iMac4s), 2013, pp. 514–517, doi:10.1109/iMac4s.2013.6526467.
[4] V.K. Quy, N.T. Ban, V.H. Nam, D.M. Tuan, N.D. Han, Survey of recent routing metrics and protocols for mobile ad-hoc networks, J. Commun. 14 (2) (2019) 110–120, doi:10.12720/jcm.14.2.110-120.
[5] A. Guillen-Perez, M. Cano, Flying ad hoc networks: a new domain for network communications, Sensors (Basel) 18 (10) (2018), doi:10.3390/s18103571.
[6] N. Saputro, K. Akkaya, S. Uluagac, Supporting seamless connectivity in drone-assisted intelligent transportation systems, in: 2018 IEEE 43rd Conference on Local Computer Networks Workshops (LCN Workshops), 2018, pp. 110–116, doi:10.1109/LCNW.2018.8628496.
[7] N. Saputro, K. Akkaya, R. Algin, S. Uluagac, Drone-assisted multi-purpose roadside units for intelligent transportation systems, in: 2018 IEEE 88th Vehicular Technology Conference (VTC-Fall), 2018, pp. 1–5, doi:10.1109/VTCFall.2018.8690977.
[8] M.K. Singh, S.I. Amin, S.A. Imam, V.K. Sachan, A. Choudhary, A survey of wireless sensor network and its types, in: 2018 International Conference on Advances in Computing, Communication Control and Networking (ICACCCN), 2018, pp. 326–330, doi:10.1109/ICACCCN.2018.8748710.
[9] IEEE standard for information technology–telecommunications and information exchange between systems–local and metropolitan area networks–specific requirements part 11: wireless lan medium access control (mac) and physical layer (phy) specifications amendment 10: mesh networking. IEEE Std 802.11s-2011 (Amendment to IEEE Std 802.11-2007 as amended by IEEE 802.11k-2008, IEEE 802.11r-2008, IEEE 802.11y-2008, IEEE 802.11w-2009, IEEE 802.11n-2009, IEEE 802.11p-2010, IEEE 802.11z-2010, IEEE 802.11v-2011, and IEEE 802.11u-2011), 2011, pp. 1–372, doi:10.1109/IEEESTD.2011.6018236.
[10] Google, Google WiFi Mesh Router, 2020.
[11] C.J. Katila, A.D. Gianni, C. Buratti, R. Verdone, Routing protocols for video surveillance drones in ieee 802.11s wireless mesh networks, in: 2017 European Conference on Networks and Communications (EuCNC), 2017, pp. 1–5, doi:10.1109/EuCNC.2017.7980778.
[12] C. Perkins, E. Belding-Royer, S. Das, Rfc-3561: Ad hoc On-Demand Distance Vector (AoDV) Routing, 2003.
[13] G.V. Kumar, Y.V. Reddyr, D.M. Nagendra, Current research work on routing protocols for manet: a literature survey, Int. J. Comput. Sci. Eng. 2 (03) (2010) 706–713.
[14] F. Li, Y. Wang, Routing in vehicular ad hoc networks: a survey, IEEE Veh. Technol. Mag. 2 (2) (2007) 12–22.
[15] R.A. Nazib, S. Moh, Routing protocols for unmanned aerial vehicle-aided vehicular ad hoc networks: a survey, IEEE Access 8 (2020) 77535–77560.
[16] A. Nayyar, Flying adhoc network (fanets): Simulation based performance comparison of routing protocols: aodv, dsdv, dsr, olsr, aomdv and hwmp, in: 2018 International Conference on Advances in Big Data, Computing and Data Communication Systems (icABCD), 2018, pp. 1–9, doi:10.1109/ICABCD.2018.8465130.
[17] C.E. Perkins, P. Bhagwat, Highly dynamic destination-sequenced distance-vector routing (dsdv) for mobile computers, in: Proceedings of the Conference on Communications Architectures, Protocols and Applications, in: SIGCOMM'94, Association for Computing Machinery, New York, NY, USA, 1994, pp. 234–244, doi:10.1145/190314.190336.
[18] D. Johnson, D. Maltz, J. Broch, Rfc-4728: The Dynamic Source Routing Protocol (DSR) for Mobile ad hoc Networks for IPV4, 2007.
[19] M.K. Marina, S.R. Das, On-demand multipath distance vector routing in ad hoc networks, in: Proceedings Ninth International Conference on Network Protocols. ICNP 2001, 2001, pp. 14–23, doi:10.1109/ICNP.2001.992756.
[20] T. Clausen, P. Jacquet, Rfc-3626: Optimized Link State Routing Protocol (OLSR), 2003.
[21] G. Parissidis, M. Karaliopoulos, R. Baumann, T. Spyropoulos, B. Plattner, Routing Metrics for Wireless Mesh Networks, Springer, London, pp. 199–230. 10.1007/978-1-84800-909-7_8.
[22] B. Awerbuch, D. Holmer, H. Rubens, High throughput route selection in multi-rate ad hoc wireless networks, in: R. Battiti, M. Conti, R.L. Cigno (Eds.), Wireless On-Demand Network Systems, Springer Berlin Heidelberg, Berlin, Heidelberg, 2004, pp. 253–270.
[23] P. Andrzej, Z. Przemyslaw, The modified metric for self-organization wireless mesh networks, in: ITM Web Conf., 21, 2018, p. 00010, doi:10.1051/itmconf/20182100010.
[24] A. Bujari, C. Calafate, J. Cano, P. Manzoni, C. Palazzi, D. Ronzani, Flying ad-hoc network application scenarios and mobility models, Int. J. Distrib. Sens. Netw. 13 (2017), doi:10.1177/1550147717738192.
[25] G.A. Litvinov, A.V. Leonov, D.A. Korneev, Applying static mobility model in relaying network organization in mini-uavs based fanet, in: 2018Systems of Signal Synchronization, Generating and Processing in Telecommunications (SYNCHROINFO), 2018, pp. 1–7, doi:10.1109/SYNCHROINFO.2018.8456951.
[26] X. Hong, M. Gerla, G. Pei, C.-C. Chiang, A group mobility model for ad hoc wireless networks, in: Proceedings of the 2nd ACM International Workshop on Modeling, Analysis and Simulation of Wireless and Mobile Systems, in: MSWiM '99, Association for Computing Machinery, New York, NY, USA, 1999, pp. 53–60, doi:10.1145/313237.313248.
[27] M. Tropea, A.F. Santamaria, F.D. Rango, G. Potrino, Reactive flooding versus link state routing for fanet in precision agriculture, in: 2019 16th IEEE Annual Consumer Communications Networking Conference (CCNC), 2019, pp. 1–6.
[28] K. Andreev, P. Boyko, IEEE 802.11s Mesh Networking NS-3 Model, 2011. IITP, WNS3.
[29] J.D. Camp, E.W. Knightly, The ieee 802.11s extended service set mesh networking standard, IEEE Commun. Mag. 46 (8) (2008) 120–126, doi:10.1109/MCOM.2008.4597114.
[30] R.M. Abid, T. Benbrahim, S. Biaz, IEEE 802.11s wireless mesh networks for last-mile internet access: an open-source real-world indoor testbed implementation, Wirel. Sensor Netw. 2 (10) (2010) 725.
[31] H.T. Friis, A note on a simple transmission formula, Proc. IRE 34 (5) (1946) 254–256, doi:10.1109/JRPROC.1946.234568.

[32] Rec. ITU-R P.1411-9: Propagation Data and Prediction Methods for the Planning of Short-Range Outdoor Radiocommunication Systems and Radio Local Area Networks in the Frequency Range 300 MHz to 100 GHz, International Telecommunication Union, 2017.
[33] N. Lin, F. Gao, L. Zhao, A. Al-Dubai, Z. Tan, A 3d smooth random walk mobility model for fanets, in: 2019 IEEE 21st International Conference on High Performance Computing and Communications; IEEE 17th International Conference on Smart City; IEEE 5th International Conference on Data Science and Systems (HPCC/SmartCity/DSS), 2019, pp. 460–467, doi:10.1109/HPCC/SmartCity/DSS.2019.00075.
[34] B. Zhou, K. Xu, M. Gerla, Group and swarm mobility models for ad hoc network scenarios using virtual tracks, in: IEEE MILCOM 2004. Military Communications Conference, 1, IEEE, 2004, pp. 289–294.
[35] N. Aschenbruck, R. Ernst, E. Gerhards-Padilla, M. Schwamborn, Bonnmotion: a mobility scenario generation and analysis tool, in: Proceedings of the 3rd International ICST Conference on Simulation Tools and Techniques, in: SIMUTools '10, ICST (Institute for Computer Sciences, Social-Informatics and Telecommunications Engineering), Brussels, BEL, 2010, doi:10.4108/ICST.SIMUTOOLS2010.8684.
[36] U. of Bonn, Bonnmotion: A Mobility Scenario Generation and Analysis Tool, 2016. Accessed December-2019.
[37] NS-3, A Discrete Event Network Simulator, 2018.
[38] O. Bautista, Ns2mobilityhelper Class Upgrade to Support Full 3d Mobility in NS-3 Network Simulator, 2019. Accessed January-2020.
[39] O. Bautista, Visualization Tool for Mobility Scenarios in Bonnmotion Format and Tools for Modification and Conversion to NS2 Movements Format, 2019. Accessed January-2020.
[40] R. Draves, J. Padhye, B. Zill, Comparison of routing metrics for static multi-hop wireless networks, in: Proceedings of the 2004 Conference on Applications, Technologies, Architectures, and Protocols for Computer Communications, in: SIGCOMM '04, Association for Computing Machinery, New York, NY, USA, 2004, pp. 133–144, doi:10.1145/1015467.1015483.
[41] O. Bautista, Ns3 Implementation of Srftime and CRP Routing Metrics for IEEE 802.11s Mesh Standard, 2020. Accessed February-2020.